J Nanostruct 15(4): 1510-1519, Autumn 2025

RESEARCH PAPER

Simple Synthesis of Calcium Carbonate Nanoparticles and Calcium Carbonate-Silver Nanocomposites with Three Various Micro-Wave, Ultrasonic Waves and Hydrothermal Methods

Abdolmotaleb Hajati [1]*, *Davood Ghanbari* [2]

[1] *Mining Engineering Department, Arak University of Technology , Arak, Iran*

[2] *Department of Science, Arak University of Technology, Arak, Iran*

ARTICLE INFO

Article History:
Received 05 June 2025
Accepted 10 August 2025
Published 01 October 2025

Keywords:
Calcium carbonate
E-coli bacteria
Nanocomposite
Photocatalyst

ABSTRACT

In this work $CaCO_3$ nanoparticles and $CaCO_3$-Ag nanocomposites were synthesized from calcium carbonate mine by three various procedures. Hydrothermal, sono-chemical and micro-wave irradiation were carried out and their effects on the morphology and properties of nanoparticles were studied. Photocatalytic performance was estimated for degradation of methyl orange toxic dye under visible light and indicates high decolorization. Results indicate that, $CaCO_3$-Ag nanocomposite show photocatalytic suitable efficiency. The presence of Ag in the nanocomposite facilitates photocatalytic decolorization reaction. The effect of different parameters such as amount, radiation time and source of photon was also investigated. This work presents a cost-effective photocatalyst for purification of toxic aromatic dyes from water. Antibacterial activity was investigated by degradation of E-coli bacteria in the presence of $CaCO_3$–Ag nanocomposite.

How to cite this article
Hajati A., Ghanbari D. Simple Synthesis of Calcium Carbonate Nanoparticles and Calcium Carbonate-Silver Nanocomposites with Three Various Micro-Wave, Ultrasonic Waves and Hydrothermal Methods . J Nanostruct, 2025; 15(4):1510-1519. DOI: 10.22052/JNS.2025.04.002

INTRODUCTION

Calcium carbonate ($CaCO_3$) is the most abundant mineral in nature, which makes it a cheap and inorganic substance. Synthetic forms of $CaCO_3$ in oil, paints, paper, plastics, coatings, environmentally friendly materials, calcium-enriched foods, Portland cement and steelmaking, as agricultural inputs for soil amendment and food additives in soy milk and products Dairy has many uses. In addition to various industrial applications as an alloying material, calcium is also an essential biological element found in bones, teeth, and shells. Calcium carbonate nanoparticles are synthesized through precipitation of calcium nitrate and saturated sodium carbonate solution. Catalysts activated in the presence of light are known as photocatalysts, that is one of application of advanced oxidation processes (AOP) and has been widely used in many fields, such as settling the energy problem, destruction the synthetic dyes, eliminating greenhouse effect and so on. The use of nano-scale photocatalysts increases the photocatalytic efficiency but nano size substances can cause irreparable environmental hazard. Due to of the nanoparticles size, separating this materials upon completion of the photocatalytic reaction

* *Corresponding Author Email: am_hajati@arakut.ac.ir*

via ordinary filtration procedures are impractical. Unique features emerge when the particle size is less than critical size; this size depends on the nature of the material. Various photocatalytic are prepared and investigated for potential application for the decay of biological wastes. Photocatalytic materials reduce organic compounds by advance oxidation process. Hospitals treat microbial contaminated wastewater by either way such as autoclaving and irradiation methods for remove or inactivate prior to discharge. All these systems have their own advantages and limitations. In the last decade, photocatalysis, a new technology which is based on advance oxidation processes and is capable of producing various reactive kinds such as oxygen radicals and hydroxyl radicals have attracted the attention for the degradation of bio-organic wastes [1-10].

This research purpose is presentation an efficient photocatalysts for degradation dyes under ultra violet or sun light radiation. In this work, nanocomposite was used to degrade methyl orange dye. Photocatalytic reactions are carried out in a heterogeneous system with solvent; Finding a low-cost photocatalyst material is a very important factor in selecting precursors for industrial acceptance.

MATERIALS AND METHODS

Materials

XRD patterns were recorded by a Philips, X-ray diffractometer using Ni-filtered CuKα radiation. Size and morphology of nanoparticles were investigated via scanning electron microscopy (model MIRA TESCAN). The golden thin film was used as a conductive coating on the surface of the samples (Prevent the accumulation of electrical charge and make better contrast(. Magnetic attributes were studied using a vibrating sample magnetometer (VSM) at room temperature in an applied magnetic field sweeping between ±10000 Oe.

About 100 kg of samples in three types with different grades of RS-A (Rostami Sayeh Seng- Kar Front A (Abbasabad Mahallat)), RS-B (Rostami Sayeh Seng- Kar Front B (Abbas Abad Mahallat)) and MR (Mehrgan Mine) - Hamedan) was prepared from the mine and sent to Arak University of Technology. The size of most of the larger stones brought was 15 cm. With the help of jaw and roller crusher, all three samples were converted into millimeter dimensions.

Preparation of calcium carbonate from calcium oxide

In the first step calcium carbonate was clacinated at 700 ^{0}C for preparation of calcium oxide. Then 20 grams of prepared calcium oxide was added little by little in distilled water and stirred well. At this stage, calcium oxide is dissolved in water and impurities remain. This step is considered a purification step. A small amount of calcium oxide can be dissolved in distilled water and produce calcium hydroxide. Carbonation is a chemical reaction in which calcium hydroxide reacts with carbon dioxide according to the following formula and forms insoluble calcium carbonate. Impurities and large amounts of calcium oxide in the previous step were not dissolved in distilled water and settled. These solids were separated from the resulting solution. To form calcium carbonate precipitate, we added CO_2 to the desired solution

CERTIFICATE OF ANALYSIS 1399-9080

1399-9080

Element	SiO2	Al2O3	BaO	CaO	Fe2O3	K2O	MgO	MnO	Na2O	P2O5	SO3	TiO2	LOI	Sr
Unit	%	%	%	%	%	%	%	%	%	%	%	%	%	%
DL	0.05	0.05	0.05	0.05	0.05	0.05	0.05	0.05	0.05	0.05	0.05	0.05	0.05	0.05
Scheme	WR-01	WR-01	WR-01	WR-01	WR-01	WR-01	WR-01	WR-01	WR-01	WR-01	WR-01	WR-01	WR-01	WR-01
CO														
CO														
MR	0.45	0.10	<	56.02	0.13	<	0.33	<	0.06	<	0.05	<	42.78	0.07
RS-A	0.36	0.09	<	55.53	0.07	<	0.23	<	<	<	0.09	<	43.63	<
RS-B	2.41	0.65	<	53.78	0.29	0.11	0.35	<	0.10	<	0.05	<	42.26	<

Fig. 1. Phase characterization of three different precursors (MR, RS-A, RS-B).

and gave the desired carbon dioxide gas to the desired solution, solid carbon dioxide (dry ice): We added dry ice to the solution and used a magnet to stir the solution.

Preparation of calcium carbonate from recrystallization

2 g of rock sample was dissolved with 3 ml of acid (HCl). Solving the sample with acid and doing

CERTIFICATE OF ANALYSIS 1399-9080

1399-9080

Element	Ag	Al	As	Ba	Be	Bi	Ca	Cd	Ce	Co	Cr	Cs	Cu	Dy	Er	Eu	Fe	Gd	Hf	In
DL	0.1	100	0.1	1	0.2	0.1	100	0.1	0.5	1	1	0.5	1	0.02	0.05	0.1	100	0.05	0.5	0.5
Unit	ppm	ppm	ppm	ppm	ppm	ppm	ppm	ppm	ppm	ppm	ppm	ppm	ppm	ppm	ppm	ppm	ppm	ppm	ppm	ppm
Method	MMS-01	MMS-01	MMS-01	MMS-01	MMS-01	MMS-01	MMS-01	MMS-01	MMS-01	MMS-01	MMS-01	MMS-01	MMS-01	MMS-01	MMS-01	MMS-01	MMS-01	MMS-01	MMS-01	MMS-01
CO																				
CO																				
MR	0.6	714	6.2	10	<0.2	<0.1	>10%	0.3	1	<1	100	<0.5	29	0.5	<0.05	<0.1	674	0.77	0.57	<0.5
RS-A	0.5	400	8.8	49	0.5	<0.1	>10%	0.2	1	<1	65	<0.5	20	0.42	<0.05	<0.1	517	0.74	0.53	<0.5
RS-B	0.4	3435	10.7	37	0.7	<0.1	>10%	0.1	4	<1	30	3.2	44	0.58	0.07	<0.1	1963	0.89	0.63	<0.5

CERTIFICATE OF ANALYSIS 1399-9080

1399-9080

Element	K	La	Li	Lu	Mg	Mn	Mo	Na	Nb	Nd	Ni	P	Pb	Pr	Rb	S	Sb	Sc	Se	Sm	Sn	Sr
DL	100	1	1	0.1	100	5	0.1	100	1	0.5	1	10	1	0.05	1	50	0.5	0.5	0.5	0.02	0.1	1
Unit	ppm	ppm	ppm	ppm	ppm	ppm	ppm	ppm	ppm	ppm	ppm	ppm	ppm	ppm	ppm	ppm	ppm	ppm	ppm	ppm	ppm	ppm
Method	MMS-01	MMS-01	MMS-01	MMS-01	MMS-01	MMS-01	MMS-01	MMS-01	MMS-01	MMS-01	MMS-01	MMS-01	MMS-01	MMS-01	MMS-01	MMS-01	MMS-01	MMS-01	MMS-01	MMS-01	MMS-01	MMS-01
CO																						
CO																						
MR	197	2	<1	<0.1	2115	<5	<0.1	<100	<1	2.9	1	107	40	0.31	<1	159	<0.5	0.6	3.37	<0.02	0.7	701
RS-A	105	2	<1	<0.1	1391	<5	<0.1	<100	<1	2.6	<1	<10	20	0.2	<1	547	<0.5	0.6	4.36	<0.02	0.7	379
RS-B	1012	3	3	<0.1	1985	24	<0.1	278	<1	4	<1	36	6	0.55	3	563	<0.5	1.2	2.51	<0.02	1.8	438

CERTIFICATE OF ANALYSIS

1399-9080

Element	Ta	Tb	Te	Th	Ti	Tl	Tm	U	V	W	Y	Yb	Zn	Zr
DL	0.1	0.1	0.1	0.1	10	0.1	0.1	0.1	1	1	0.5	0.05	1	5
Unit	ppm	ppm	ppm	ppm	ppm	ppm	ppm	ppm	ppm	ppm	ppm	ppm	ppm	ppm
Method	MMS-01	MMS-01	MMS-01	MMS-01	MMS-01	MMS-01	MMS-01	MMS-01	MMS-01	MMS-01	MMS-01	MMS-01	MMS-01	MMS-01
CO														
CO														
MR	0.2	<0.1	<0.1	<0.1	<10	<0.1	<0.1	2.6	7	<1	1.1	1.3	12	<5
RS-A	0.2	<0.1	<0.1	<0.1	<10	<0.1	<0.1	0.1	2	<1	<0.5	1.2	13	<5
RS-B	0.22	<0.1	<0.1	<0.1	82	<0.1	<0.1	0.3	7	<1	1.2	1.3	18	6

Fig. 2. Elemental characterization of three different precursors (MR, RS-A, RS-B).

the opposite reaction, some impurity is formed, and due to the fact that calcium chloride is dissolved in the acid, the impurities settle and are separated from the above solution with the help of filter paper.

Sodium hydroxide was used to neutralize the solution, it was added little by little to the solution containing the sample and checked until the solution turned from acidic to neutral. 25 ml of the prepared sodium carbonate (or ammonium carbonate) 0.1M solution was added to these two solutions separately while stirring. Then it was placed in the microwave for 10 minutes (On:20s, Off:20s) . Then it was placed in a centrifuge and the deposited sediment was separated and placed in the oven.

The previous steps were repeated and ammonium carbonate (or sodium carbonate) was added to both solutions and placed inside the hydrothermal (200 ^{0}C, 12 h). Then it was placed in a centrifuge and the deposited sediment was separated and placed in the oven.

On the third reaction the solutions was placed in the ultrasonic device (1200W, 60 min). Then it was placed in a centrifuge and the deposited sediment was separated and placed in the oven.

In this method, all steps are similar to the second method, with the difference that instead of sodium carbonate, ammonium carbonate is used for sedimentation. As results confirm ammonium carbonate show higher purity compare to other precipitating agents.

By using all three methods (microwave, hydrothermal and ultrasonic) and by adding ammonium carbonate solution (ammonium carbonate in distilled water: 0.1 M) the following reaction occurs and finally calcium carbonate precipitate is formed which is in the form of nanoparticles and has no impurities is.

$$CaCl_2 + (NH_4)_2CO_3 \rightarrow CaCO_3 + 2NH_4Cl \quad (1)$$

For preparation of nanocomposite 1 g of calcium carbonate nanoparticles that were achieved by microwave method was dispersed in 200 ml of distilled water, after that 1 g of silver nitrate was dissolved to the solution, after 5 h of mixing, 1 g of lactose as a capping agent was added to the solution, finally by heating at 90 ^{0}C, ammonia (10M) as a reducing agent was added, Final precipitated was washed and dried at oven (60 ^{0}C) for 24 h.

RESULTS AND DISCUSSION

Fig. 1 shows phase characterization of carbonate calcium precursor. Elemental characterizations of three different precursors (MR, RS-A, RS-B) are shown in Fig. 2. Both analysis show high purity of the precursor, for obtaining higher purity this precursor was dissolved and was precipitated under different conditions.

Fig. 3 illustrate the X-ray diffraction patterns of pre-cursor nanocrystals obtained from mine, all the diffraction peaks at 2θ values of 23°, 29°, 36°,

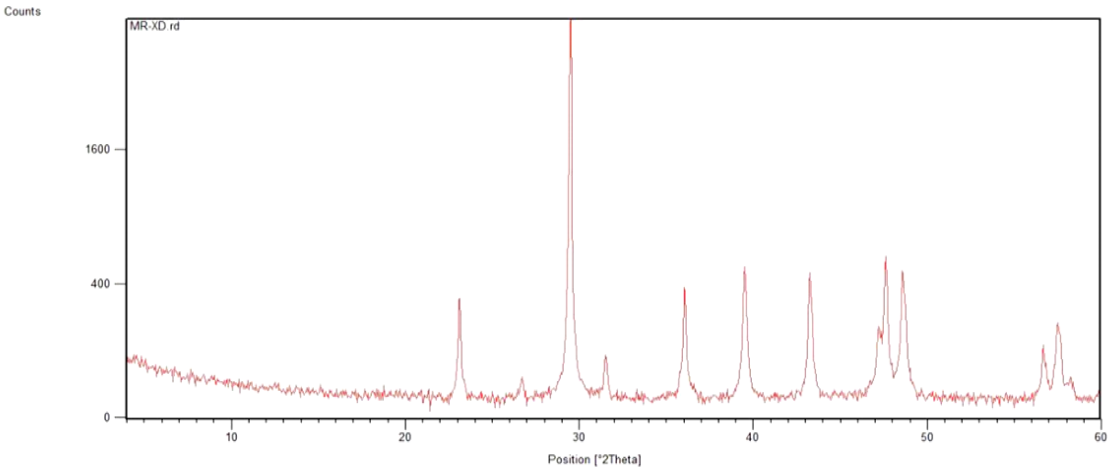

Fig. 3. XRD pattern of calcium carbonate precursor.

39° , 43°, 47°, 49° and 57° are indexed to lattice planes of cubic $CaCO_3$ spinel structure (JCPDS NO. 05-0586). It shows the results obtained from X-ray diffraction pattern that approve high percent purity (about 99 percent) of the precursor.

Fig. 4 illustrates XRD pattern of calcium carbonate nanoparticles obtained by sono-chemical method. As we expected by ultrasound irradiation, nanoparticles are synthesized and because of power of collapsing of bubbles crytallinty was decreased.

Fig. 5 shows XRD pattern of calcium carbonate nanoparticles synthesized under micro-wave irradiation. All the diffraction peaks are indexed to pure calcite structure (JCPDS NO. 72-1652). Results confirm microwave irradiation improve

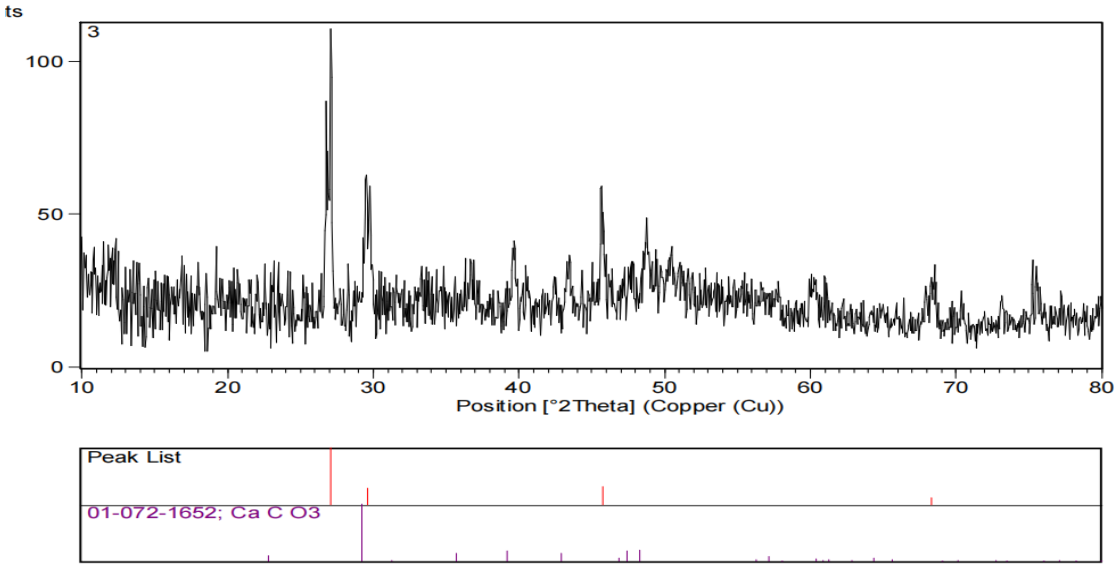

Fig. 4. XRD pattern of calcium carbonate nanoparticles obtained by sono-chemical method.

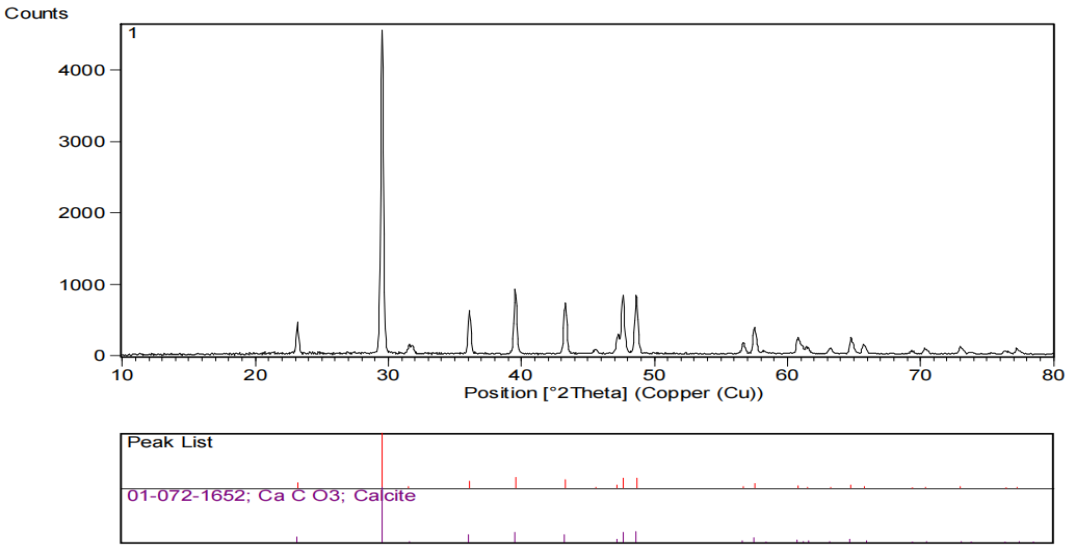

Fig. 5. XRD pattern of calcium carbonate nanoparticles synthesized under micro-wave irradiation.

growth and crystallinty. Fig. 6 depicts XRD pattern of calcium carbonate nanoparticles synthesized with hydrothermal procedure. By hyrothermal method, both calcite phase (JCPDS NO. 72-1652) and aragonite phase (JCPDS NO. 41-1475) were synthesized under high pressure condition.

Fig. 7 depicts FT-IR absorption of calcium carbonate nanoparticles synthesized under micro-wave irradiation. The absorption peak around 700 cm^{-1} is ascribed to the Ca–O bonds, the absorption peaks about 3420 cm^{-1} is ascribed to O–H bonds on the surface of nanoparticles. The bonds for each

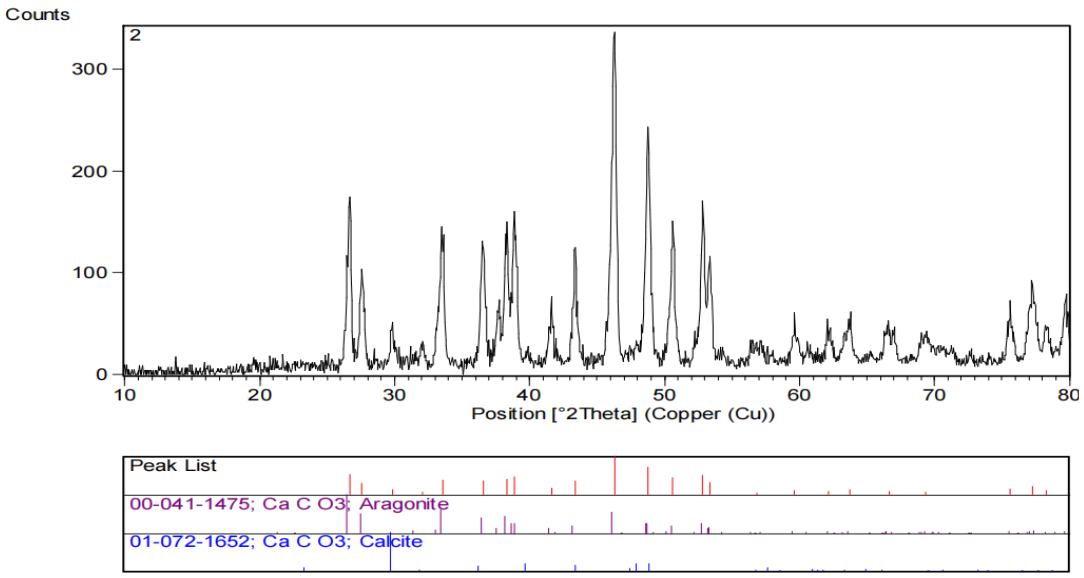

Fig. 6. XRD pattern of calcium carbonate nanoparticles synthesized with hydrothermal procedure.

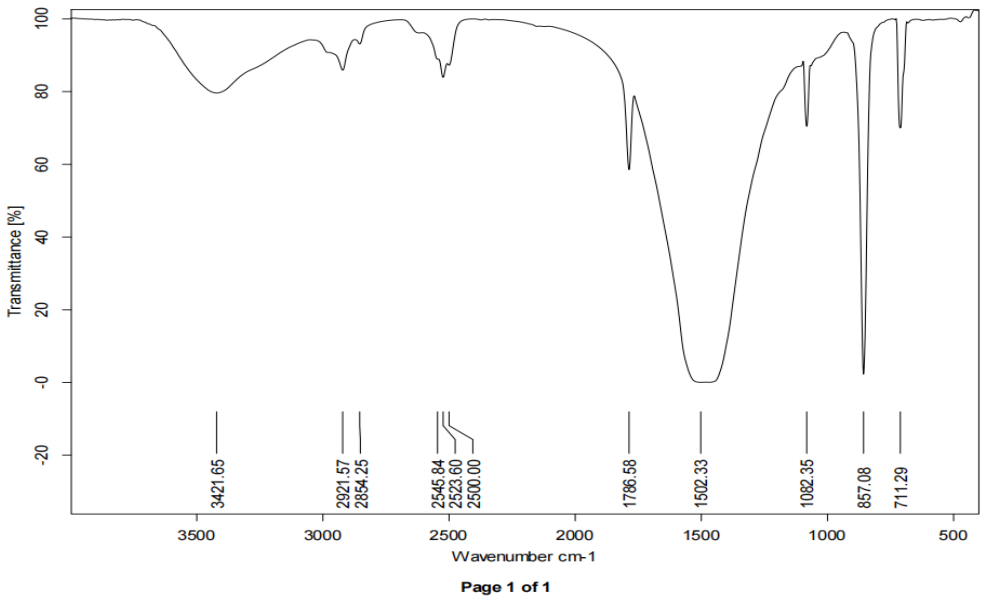

Fig. 7. FT-IR absorption of calcium carbonate nanoparticles synthesized under micro-wave irradiation.

absorptions peak are shown in the figure. A sharp peak near 900 cm^{-1} is assigned to C–O vibration. The absorption about 1600 cm^{-1} is assigned to C=O vibration and the absorption peaks at 2900 cm^{-1}

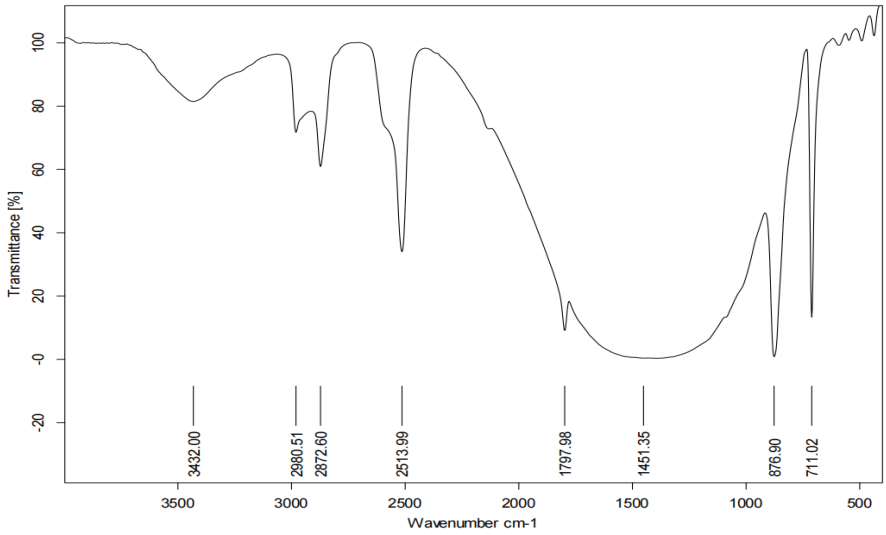

Fig. 8. FT-IR absorption of calcium carbonate nanoparticles synthesized with hydrothermal procedure.

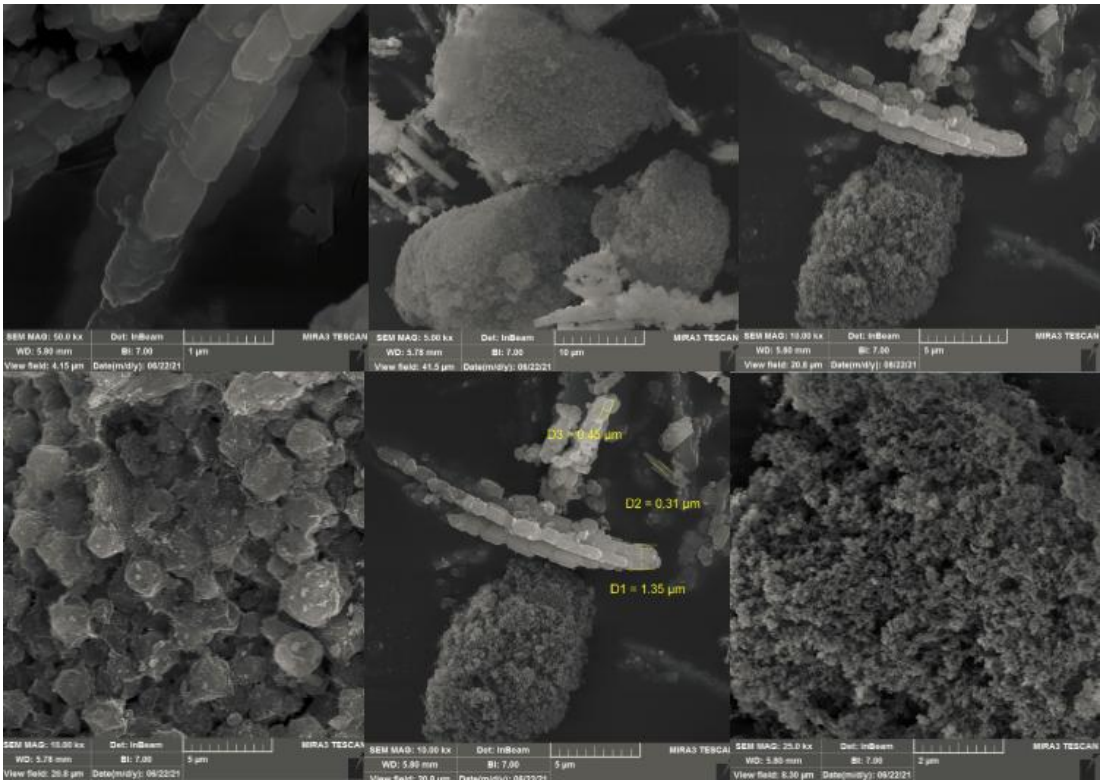

Fig. 9. SEM images of calcium carbonate nanoparticles prepared under micro-wave irradiations.

is assigned to C–H vibration. FT-IR absorption of calcium carbonate nanoparticles synthesized with hydrothermal procedure is shown in Fig. 8. Results show the same characterization absorption peaks in the same regions.

Morphological characteristics of the samples, the as-prepared pure calcium carbonate nanoparticles prepared using different methods were investigated by scanning electron microscopy. SEM images of $CaCO_3$ nanoparticles are shown in Fig. 9. According to images, the average particles size about 80 nm was estimated. It seems that the use of microwave irradiation is more suitable for the preparation of pure nanoparticles. Hot spots that were prepared by microwave (or ultrasonic) methods prevent agglomeration and leads to smaller nanoparticles. SEM images of $CaCO_3$-Ag nanocomposite are illustrated in Fig. 10 that approve average particle size are less than 100 nm. Cubic nanostructures with some agglomeration were synthesized, results approve by hydrothermal reaction (high pressure and temperature) preferential growth was observed; Images confirm cubic nanostructures has suitable surface to volume ratio for catalytic applications.

The photocatalytic activity of the $CaCO_3$–Ag nanocomposite was evaluated. Fig. 11 illustrates the effect of radiation time on methyl orange photo-degradation in presence of $CaCO_3$–Ag nanocomposite. According to the energy gap of (Eg = 2.82 eV), visible light can cause the formation of electron-hole pairs in the matter. The conduction band position is lower (less negative) than the oxygen redox potential, therefore the electrons in the conduction band cannot to produce superoxide anions but via hydrogen peroxide produced hydroxyl radicals. Also, the valence band position is lower than the water oxidation potential and the formation of radical hydroxyl. Therefore, has a high oxidation capability and is able to oxidize water and create active radical species.

The relative location of the conduction bands and valence bands of materials, create ideal conditions for the transfer of electrons Therefore, the amount of hydrogen peroxide in the photocatalyst atmosphere increases. Hydrogen peroxide reacts with the electron and leads to the formation of radical hydroxyl. With increasing radical production, photocatalytic degradation increases.

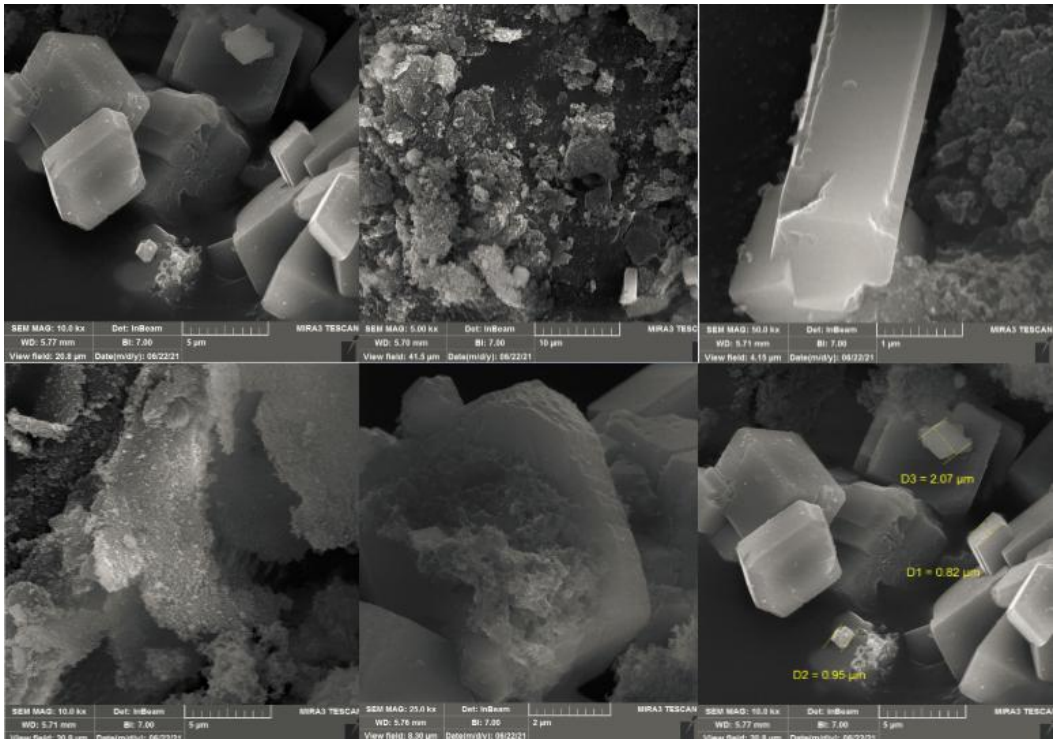

Fig. 10. SEM images of calcium carbonate-silver nanocomposite synthesized with hydrothermal procedure.

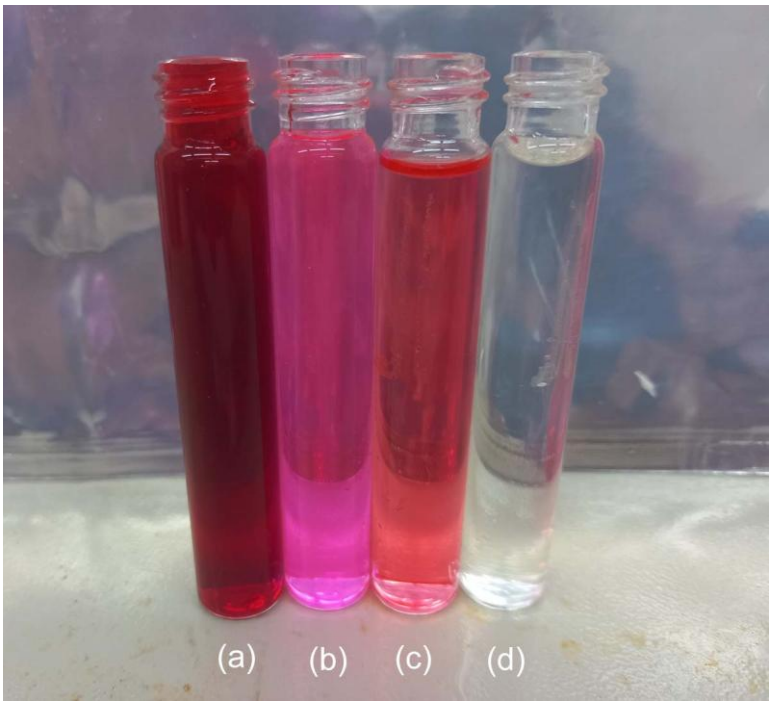

Fig. 11. Photo degradation of methyl orange (a) 0 min (b) 30 min (c) 60 min (d) 120 min.

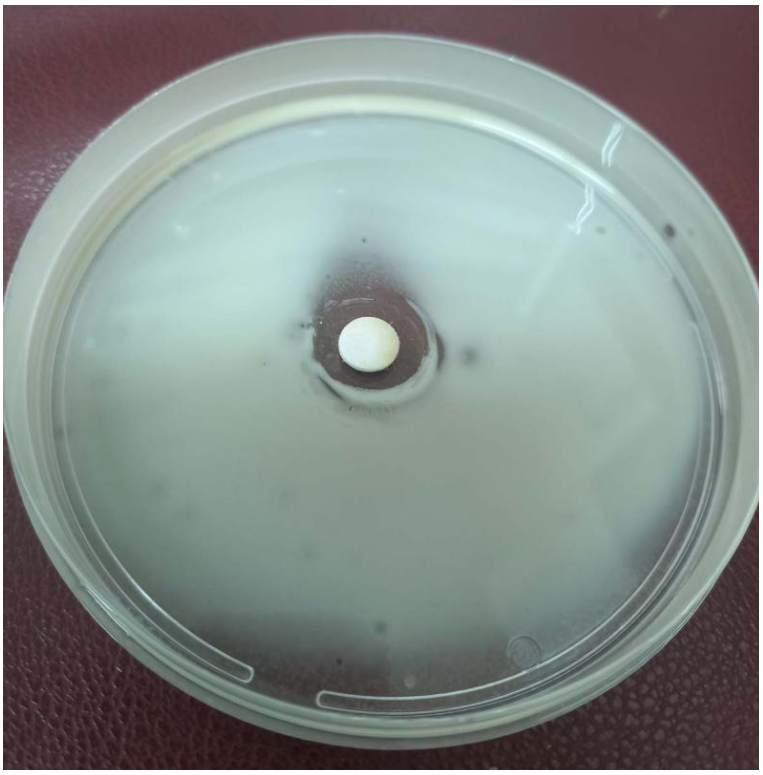

Fig. 12. Antibacterial activity against E-coli bacteria.

Mechanisms of degradation could be on the following mentioned, first of all oxidative stress induction; in which the active radicals, cause the oxidation process in the cells that leads destroy proteins, reduce the activity of special enzyme, and finally interact with DNA. Maybe metal ions are infiltrate into the cell and directly interact with the –NH , –SH and –COOH group of nucleic acid and protein. Inactivation of bacteria's via decreasing the important cellular metabolism such as energy, amino acid, carbohydrate, protein, and nucleotide without oxidative stress infusion [11-13]. As shown in the Figs. 12 with the creation of composites, the antibacterial properties have been improved due to the simultaneous presence of active radicals and silver.

CONCLUSION

$CaCO_3$ and $CaCO_3$-Ag nanocomposites were synthesized by various procedures, hydrothermal, sono-chemical and micro-wave irradiation. Photocatalytic performance was appraised for degradation of methyl orange dye under visible light. The photocatalytic degradation of the $CaCO_3$-Ag nanocomposite was examined by the de-coloration reaction of methyl orange in an aqueous solution. This work introduces a novel smart photocatalyst for purification of toxic aromatic dyes from water.

CONFLICT OF INTEREST

The authors declare that there is no conflict of interests regarding the publication of this manuscript.

REFERENCES

1. Seyghalkar H, Sabet M, Salavati-Niasari M. Synthesis and Characterization of Cadmium Sulfide Nanoparticles via a Simple Thermal Decompose Method. nano Online: De Gruyter; 2017.
2. Rostami A, Atashkar B. Synthesis, characterization and catalytic property of chiral oxo-vanadium (+)-pseudoephedrine complex supported on magnetic nanoparticles Fe_3O_4 in the cyanosilylation of carbonyl compounds. Catal Commun. 2015;58:80-84.
3. Salavati-Niasari M, Sabet M, Fard ZA, Saberyan K, Mostafa Hosseinpour-Mashkani S. Synthesis and Characterization of Calcium Carbonate Nanostructures via Simple Hydrothermal Method. Synthesis and Reactivity in Inorganic, Metal-Organic, and Nano-Metal Chemistry. 2014;45(6):848-857.
4. Liendo F, Arduino M, Deorsola FA, Bensaid S. Optimization of $CaCO_3$ synthesis through the carbonation route in a packed bed reactor. Powder Technol. 2021;377:868-881.
5. Kiani A, Nabiyouni G, Masoumi S, Ghanbari D. A novel magnetic $MgFe_2O_4$–$MgTiO_3$ perovskite nanocomposite: Rapid photo-degradation of toxic dyes under visible irradiation. Composites Part B: Engineering. 2019;175:107080.
6. Petrie JR, Cooper VR, Freeland JW, Meyer TL, Zhang Z, Lutterman DA, et al. Enhanced Bifunctional Oxygen Catalysis in Strained $LaNiO_3$ Perovskites. Journal of the American Chemical Society. 2016;138(8):2488-2491.
7. Fabbri E, Nachtegaal M, Binninger T, Cheng X, Kim B-J, Durst J, et al. Dynamic surface self-reconstruction is the key of highly active perovskite nano-electrocatalysts for water splitting. Nature Materials. 2017;16(9):925-931.
8. Masoumi S, Nabiyouni G, Ghanbari D. Photo-degradation of azo dyes: photo catalyst and magnetic investigation of $CuFe_2O_4$–TiO_2 nanoparticles and nanocomposites. Journal of Materials Science: Materials in Electronics. 2016;27(9):9962-9975.
9. Metzler DM, Li M, Erdem A, Huang CP. Responses of algae to photocatalytic nano-TiO_2 particles with an emphasis on the effect of particle size. Chem Eng J. 2011;170(2-3):538-546.
10. Eskandari N, Nabiyouni G, Masoumi S, Ghanbari D. Preparation of a new magnetic and photo-catalyst $CoFe_2O_4$–$SrTiO_3$ perovskite nanocomposite for photo-degradation of toxic dyes under short time visible irradiation. Composites Part B: Engineering. 2019;176:107343.
11. Chung K-T. The significance of azo-reduction in the mutagenesis and carcinogenesis of azo dyes. Mutation Research/Reviews in Genetic Toxicology. 1983;114(3):269-281.
12. Stylidi M. Pathways of solar light-induced photocatalytic degradation of azo dyes in aqueous TiO2 suspensions. Applied Catalysis B: Environmental. 2003;40(4):271-286.
13. Zinatloo-Ajabshir S, Esfahani MH, Marjerrison CA, Greedan J, Behzad M. Enhanced electrochemical hydrogen storage performance of lanthanum zirconium oxide ceramic microstructures synthesized by a simple approach. Ceram Int. 2023;49(23):37415-37422.